

00  
1004  
CJ  
U1

TECH LIBRARY KAFB, NM  
0344947

AF130  
JUL 1961  
AF 6011

TECH LIBRARY KAFB, NM  
1 1000000000 0000000000 0000000000 0000000000



## TECHNICAL NOTE NO. 1681

CRITICAL SHEAR STRESS OF AN INFINITELY  
LONG PLATE IN THE PLASTIC REGION

By Elbridge Z. Stowell

## SUMMARY

The plasticity reduction factor in the formula for the buckling stress of a long plate under uniform shear has been computed from the properties of the stress-strain curve for the material. Some limited tests on the shear buckling of 24S-O aluminum-alloy plates in the plastic region tend to confirm the value of the reduction factor predicted by the theory. Restraint against rotation along the edges of the plate has little or no effect upon the value of the reduction factor according to theoretical calculation.

## INTRODUCTION

The problem of computing the critical shear stress for an infinitely long plate with edges elastically restrained against rotation was solved for the elastic stress range in reference 1. The theory of reference 1 is no longer applicable, however, in cases where buckling occurs beyond the elastic range; in such cases, the theory must be modified to allow for curvature of the stress-strain curve. The problem consists in the computation of the plasticity reduction factor  $\eta$  in terms of the properties of the stress-strain curve for the material.

The general equations for the buckling of a thin plate under combined compression and shear in the plane of the plate were derived in reference 2. Upon the assumption that the plate remains in the plastic state during buckling, the differential equation of equilibrium of the plate was derived, together with the corresponding expressions for the variations in energy at buckling. These general expressions were then applied to the case of a plate in which one of the compressive forces and the shear force were zero, that is, to a plate under simple compression.

The same general expressions may also be applied to the case of a plate under pure shear in the plane of the plate by setting both compressive forces equal to zero. This application has been made in the present paper.

## RESULTS

Theoretical results.— The plate is assumed to be infinitely long with side edges elastically restrained against rotation. The applied shear stress is assumed to be uniformly distributed and, as in reference 2, no unloading of the plate is assumed to occur during buckling. By virtue of these assumptions, the plate remains in the plastic state during buckling and the relations developed in reference 2 apply.

The procedure followed is to employ the same deflection surface in the energy expressions for the plastic case that was used in reference 1 for the elastic case. From the resulting expressions the approximate value of the critical shear stress in the plastic region is computed. The expression for the critical shear stress in such a case is

$$\tau = \eta \frac{\pi^2 k_s E t^2}{12 (1 - \mu^2) b^2}$$

in which

$\tau$	critical shear stress
$k_s$	coefficient depending upon conditions of edge restraint and shape of plate
$t$	thickness of plate
$b$	width of plate
$E$	Young's modulus
$\mu$	Poisson's ratio
$\eta$	coefficient which allows for reduction in shear stress in plastic range

The value of the wave length required to make the critical shear stress a minimum is found and is substituted in the expression for the critical shear stress, which is then known in terms of the angle of the waves, the magnitude of the elastic restraint, and the plasticity coefficients. Division of this expression for the critical shear stress by the corresponding approximate expression in the elastic range gives the value of the coefficient  $\eta$  to a closer approximation than either of the individual critical stresses.

The coefficient  $\eta$  is given formally in the appendix as a function of the angle of the waves  $\phi$ , the magnitude of the elastic restraint  $\epsilon$ ,

and the plasticity coefficients  $E_s/E$  and  $C_3$ . The resulting equation is

$$\eta = \frac{E_s \sin 2\phi_0}{E \sin 2\phi} \frac{2 \sqrt{f_1(\epsilon)} \sqrt{1 - \frac{1-C_3}{2} \sin^2 2\phi} + 2[1 + 2 \sin^2 \phi - (1-C_3) \cos^2 \phi] f_2(\epsilon)}{2 \sqrt{f_1(\epsilon)} + 2(1 + 2 \sin^2 \phi_0) f_2(\epsilon)} \quad (1)$$

where

$E_s$  secant modulus of material

$f_1(\epsilon), f_2(\epsilon)$  functions of elastic restraint  $\epsilon$

$C_3$  plasticity coefficient

$\phi_0$  wave angle in elastic range

$$\phi = \frac{1}{2} \cos^{-1} \frac{(3 - C_3) f_2(\epsilon)}{\frac{2 \sqrt{f_1(\epsilon)}}{\sqrt{1 - \frac{1-C_3}{2} \sin^2 2\phi}} + (3 + C_3) f_2(\epsilon)}$$

The angle of the waves  $\phi$  is that angle which will make the critical shear stress a minimum. As soon as the magnitude of the elastic restraint is selected, the angle of the waves, and therefore  $\eta$ , may be computed for any stress.

Computations of  $\eta$  were made for a plate of 24S-T aluminum alloy in the cases where the edges of the plate were simply supported and clamped. The procedures used are given in detail in the appendix. The calculations with both edge conditions resulted in substantially the same curve, shown in figure 1. Curves of  $\eta = \frac{E_s}{E}$  and  $\eta = \frac{E_t}{E}$  as obtained for compression in reference 2 are included for comparison.

Experimental check.— The critical shear stress of eight long plates of 24S-0 aluminum alloy has been measured in the plastic region by Gerard (reference 3). An attempt was made to secure a clamped condition along the edges and buckling was determined by the difference in strain on opposite sides of the sheet as measured with electrical gages. Gerard's data are represented by the test points in figure 2. The solid-line curve of figure 2 gives the theoretical values of  $\eta$  as computed by equation (1) from the axial stress-strain curve supplied by Gerard for 24S-0 aluminum alloy in reference 3. This theoretical curve confirms the trend of the experimental points in a satisfactory manner, although it lies in the upper part of the scatter band.

In reference 3 Gerard suggested that the shear secant modulus be used as the effective modulus for a long plate under shear. Gerard's assumption is, from equation (2) of reference 3,

$$\eta = \frac{G_s}{G}$$

where the  $G$ 's refer to the slope of a shear stress-strain curve derived from the axial stress-strain curve. The dash-line curve in figure 2, which was computed from figure 8 of reference 3, shows the value of  $\eta$  that results from this suggestion. The agreement with the solid-line curve, which represents the values of  $\eta$  computed from the theory of the present paper, is seen to be fair.

The necessary conditions for use of the shear secant modulus, however, should be examined further. In the appendix, equation (1) is shown to reduce to the form

$$\eta = \text{Constant} \frac{E_s}{E}$$

if  $C_3$  is constant. For Gerard's curve for 24S-0 aluminum alloy the requirement for a constant  $C_3$  is closely fulfilled. When the value of  $\eta$  is computed from equation (1), it is found that

$$\eta = 0.89 \frac{E_s}{E}$$

This relation is plotted as the solid line in figure 2. Results of the calculation are also given in a more familiar form in figure 3.

Caution should be employed in generalizing the use of the shear secant modulus to materials, such as 24S-T aluminum alloy, for which  $C_3$  is not a constant in the plastic range. The upper curve in

figure 1 represents  $E_g/E$  for 24S-T aluminum alloy and therefore describes the axial stress-strain curve for that material. The center curve, which represents  $\eta$ , cannot be obtained from the upper curve by multiplying the ordinates by a constant factor throughout the plastic range; therefore  $\eta$  for this material is not the shear secant modulus.

#### CONCLUSIONS

The theory of plastic buckling previously reported has been applied to the determination of the plasticity reduction factor in the formula for the buckling stress of a long plate under uniform shear from the properties of the stress-strain curve for the material. Some limited data on the shear buckling of 24S-O aluminum-alloy plates in the plastic region tend to confirm the value of the reduction factor predicted by the theory. The theory indicates that restraint against rotation along the edges of the plate has little or no effect on the value of the reduction factor.

Langley Aeronautical Laboratory  
National Advisory Committee for Aeronautics  
Langley Field, Va., May 24, 1948

## APPENDIX

## ANALYSIS

General theory.—Reference 2 shows that for a plate under shear alone the work  $T$  done on the plate, expressed in a Cartesian  $(x', y')$  system, is

$$T = \tau t \int_{-\frac{b}{2}}^{\frac{b}{2}} \int_{-\frac{\lambda}{2}}^{\frac{\lambda}{2}} \frac{\partial w}{\partial x'} \frac{\partial w}{\partial y'} dx' dy' \quad (2)$$

where

- $\tau$  applied shear stress  
 $w$  deflection of plate at  $(x', y')$   
 $\lambda$  half-wave length

The expression for the strain energy in the plate  $V_1$ , from reference 2, is

$$V_1 = \frac{D'}{2} \int_{-\frac{b}{2}}^{\frac{b}{2}} \int_{-\frac{\lambda}{2}}^{\frac{\lambda}{2}} \left\{ \left( \frac{\partial^2 w}{\partial x'^2} \right)^2 + C_3 \left[ \left( \frac{\partial^2 w}{\partial x' \partial y'} \right)^2 + \frac{\partial^2 w}{\partial x'^2} \frac{\partial^2 w}{\partial y'^2} \right] + \left( \frac{\partial^2 w}{\partial y'^2} \right)^2 \right\} dx' dy' \quad (3)$$

where

$$C_3 = \frac{1}{2} + \frac{1}{2} \frac{E_t}{E_s}$$

$$D' = t^3 \frac{E_s}{9}$$

$E_t$  tangent modulus of material

If, in addition, the plate has equal elastic restraints  $e$  against rotation along the side edges, the strain energy in these restraints  $V_2$  is, from reference 2,

$$V_2 = \frac{D^* \epsilon}{2b} \int_{-\frac{\lambda}{2}}^{\frac{\lambda}{2}} \left[ \frac{\partial w}{\partial y^*} \right]_{y^* = \frac{b}{2}}^2 dx^* + \frac{D^* \epsilon}{2b} \int_{-\frac{\lambda}{2}}^{\frac{\lambda}{2}} \left[ \frac{\partial w}{\partial y^*} \right]_{y^* = -\frac{b}{2}}^2 dx^* \quad (4)$$

Let a more suitable oblique coordinate system be defined by

$$\left. \begin{aligned} x &= x^* + y^* \tan \phi \\ y &= \frac{y^*}{\cos \phi} \end{aligned} \right\} \quad (5)$$

as in reference 1. (See fig. 4.)

Then  $T$ ,  $V_1$ , and  $V_2$  in the new system are

$$T = \tau t \int_{-\frac{b_1}{2}}^{\frac{b_1}{2}} \int_{-\frac{\lambda}{2}}^{\frac{\lambda}{2}} \left[ \frac{\partial w}{\partial x} \frac{\partial w}{\partial y} + \left( \frac{\partial w}{\partial x} \right)^2 \sin \phi \right] dx dy \quad (6)$$

$$\begin{aligned} V_1 &= \frac{D^*}{2 \cos \phi} \int_{-\frac{b_1}{2}}^{\frac{b_1}{2}} \int_{-\frac{\lambda}{2}}^{\frac{\lambda}{2}} \left\{ \left[ \frac{1}{\cos^2 \phi} - 2(1 - c_3) \sin^2 \phi \right] \left( \frac{\partial^2 w}{\partial x^2} \right)^2 \right. \\ &\quad + \frac{1}{\cos^2 \phi} \left( \frac{\partial^2 w}{\partial y^2} \right)^2 + \left[ 1 + 4 \tan^2 \phi - (1 - c_3) \right] \left( \frac{\partial^2 w}{\partial x \partial y} \right)^2 \\ &\quad + \left[ 1 + 2 \tan^2 \phi - (1 - c_3) \right] \frac{\partial^2 w}{\partial x^2} \frac{\partial^2 w}{\partial y^2} \\ &\quad \left. + 4 \frac{\tan \phi}{\cos \phi} \frac{\partial^2 w}{\partial x \partial y} \left[ \frac{\partial^2 w}{\partial x^2} + \frac{\partial^2 w}{\partial y^2} - (1 - c_3) \frac{\partial^2 w}{\partial x^2} \cos^2 \phi \right] \right\} dx dy \quad (7) \end{aligned}$$



$$V_2 = \frac{D'\epsilon}{2b \cos^2 \phi} \int_{-\frac{\lambda}{2}}^{\frac{\lambda}{2}} \left\{ \left[ \frac{\partial w}{\partial y} + \frac{\partial w}{\partial x} \sin \phi \right]_{y=\frac{b_1}{2}}^2 + \left[ \frac{\partial w}{\partial y} + \frac{\partial w}{\partial x} \sin \phi \right]_{y=-\frac{b_1}{2}}^2 \right\} dx \quad (8)$$

where

$$b_1 = \frac{b}{\cos \phi}$$

A comparison with the corresponding formulas in appendix B of reference 1 will show that the two groups are identical if Poisson's ratio is taken as 0.5 and if  $C_3 = 1$ ; that is, if only the elastic range is considered.

As in reference 1, the assumed deflection surface is

$$w = w_0 \left[ \frac{\pi \epsilon}{2} \left( \frac{y^2}{b_1^2} - \frac{1}{4} \right) + \left( 1 + \frac{\epsilon}{2} \right) \cos \frac{\pi y}{b_1} \right] \cos \frac{\pi x}{\lambda}$$

in which the half-wave length  $\lambda$  will be adjusted to make the critical stress a minimum. Substituting this deflection surface into expressions (6), (7), and (8) and performing the indicated integrations gives

$$T = w_0^2 \frac{\pi^2 b_1 t \sin \phi}{2\lambda} L$$

$$V_1 = w_0^2 \frac{\pi^4 D'}{4 b_1 \lambda \cos \phi} \left\{ \left( \frac{b_1}{\lambda} \right)^2 \left[ \frac{1}{\cos^2 \phi} - 2(1 - C_3) \sin^2 \phi \right] L + \frac{M}{\left( \frac{b_1 \cos \phi}{\lambda} \right)^2} + 2 \frac{1 + 2 \sin^2 \phi - (1 - C_3) \cos^2 \phi}{\cos^2 \phi} N \right\} \quad (9)$$

$$V_2 = w_0^2 \frac{\pi^2 D' \epsilon \lambda}{2 b_1^3 \cos^3 \phi}$$

where

$$L = \left( \frac{\pi^2}{120} + \frac{1}{8} - \frac{2}{\pi^2} \right) \epsilon^2 + \left( \frac{1}{2} - \frac{4}{\pi^2} \right) \epsilon + \frac{1}{2}$$

$$M = \left( \frac{1}{8} - \frac{1}{\pi^2} \right) \epsilon^2 + \left( \frac{1}{2} - \frac{4}{\pi^2} \right) \epsilon + \frac{1}{2}$$

$$N = \left( \frac{5}{24} - \frac{2}{\pi^2} \right) \epsilon^2 + \left( \frac{1}{2} - \frac{4}{\pi^2} \right) \epsilon + \frac{1}{2}$$

Setting up the equality  $T = V_1 + V_2$ , which holds at buckling, and solving for the critical shear stress  $\tau$  gives

$$\tau = \frac{1}{\sin 2\phi} \left\{ \left( \frac{b_1}{\lambda} \right)^2 \left[ \frac{1}{\cos^2 \phi} - 2(1 - C_3) \sin^2 \phi \right] + \frac{\frac{M}{L}}{\left( \frac{b_1 \cos \phi}{\lambda} \right)^2} + 2 \frac{1 + 2 \sin^2 \phi - (1 - C_3) \cos^2 \phi}{\cos^2 \phi} \frac{N}{L} + \frac{\frac{2\epsilon}{\pi^2}}{\left( \frac{b_1 \cos \phi}{\lambda} \right)_L^2} \right\} \frac{\pi^2 D^3}{b_1^2 t}$$

or, replacing  $b_1 \cos \phi$  by  $b$ , and writing  $\frac{M + \frac{2\epsilon}{\pi^2}}{L} = f_1(\epsilon)$

and  $\frac{N}{L} = f_2(\epsilon)$  yields

$$\tau = \left\{ \left( \frac{b}{\lambda} \right)^2 \left[ \frac{1}{\cos^2 \phi} - 2(1 - C_3) \sin^2 \phi \right] + \frac{f_1(\epsilon)}{\left( \frac{b}{\lambda} \right)^2} \cos^2 \phi + 2 \left[ 1 + 2 \sin^2 \phi - (1 - C_3) \cos^2 \phi \right] f_2(\epsilon) \right\} \frac{\pi^2 D^3}{b^2 t \sin 2\phi} \quad (10)$$

In the elastic range ( $C_3 = 1$ ) this expression reduces to the corresponding formula in reference 1.

The half-wave length  $\lambda$  and the wave angle  $\phi$  will adjust themselves to make  $\tau$  a minimum; that is,

$$\frac{\partial \tau}{\partial \left(\frac{b}{\lambda}\right)^2} = 0$$

which gives

$$\left(\frac{b}{\lambda}\right)^2 = \frac{\sqrt{f_1(\epsilon)} \cos^2 \phi}{\sqrt{1 - \frac{1 - C_3}{2} \sin^2 2\phi}} \quad (11)$$

from which

$$\tau_{\min} = \frac{1}{\sin 2\phi} \left\{ 2 \sqrt{f_1(\epsilon)} \sqrt{1 - \frac{1 - C_3}{2} \sin^2 2\phi} + 2 \left[ 1 + 2 \sin^2 \phi - (1 - C_3) \cos^2 \phi \right] f_2(\epsilon) \right\} \frac{\pi^2 D^3}{b^2 t} \quad (12)$$

The angle  $\phi$  is found from the relation

$$\frac{\partial \tau_{\min}}{\partial \phi} = 0$$

which gives

$$\cos 2\phi = \frac{(3 - C_3) f_2(\epsilon)}{\frac{2\sqrt{f_1(\epsilon)}}{\sqrt{1 - \frac{1 - C_3}{2} \sin^2 2\phi}} + (3 + C_3) f_2(\epsilon)} \quad (13)$$

The value of  $\phi$  is thus fixed as soon as the restraint is chosen and the value of  $E_t/E_s$  is assumed. This value of  $\phi$  is the one to be used in equation (12) for computation of the minimum critical shear stress  $\tau_{\min}$ .

In the elastic range, the corresponding minimum critical shear stress  $(\tau_0)_{\min}$  is obtained by putting  $C_3 = 1$  and  $D' = D = \frac{Et^3}{9}$  in equation (12):

$$(\tau_0)_{\min} = \frac{1}{\sin 2\phi_0} \left[ 2\sqrt{f_1(\epsilon)} + 2(1 + 2\sin^2\phi_0) f_2(\epsilon) \right] \frac{\pi^2 D}{b^2 t} \quad (14)$$

where the subscript 0 signifies that the quantity is in the elastic range. Thus, from equation (13),

$$\cos 2\phi_0 = \frac{f_2(\epsilon)}{\sqrt{f_1(\epsilon)} + 2f_2(\epsilon)} \quad (15)$$

The value of  $\eta$  is the ratio of the critical shear stress  $\tau_{\min}$  to the critical shear stress  $(\tau_0)_{\min}$  that would be obtained if the material were wholly elastic; thus

$$\eta = \frac{E_s}{E} \frac{\sin 2\phi_0}{\sin 2\phi} \frac{2\sqrt{f_1(\epsilon)} \sqrt{1 - \frac{1-C_3}{2} \sin^2 2\phi} + 2[1 + 2\sin^2\phi - (1-C_3) \cos^2\phi] f_2(\epsilon)}{2\sqrt{f_1(\epsilon)} + 2(1 + 2\sin^2\phi_0) f_2(\epsilon)}$$

The value of  $\eta$  as a function of stress will now be considered for the two extreme cases of simply supported and clamped edges:

(a) For the case of simply supported edges,

$$f_1(\epsilon) = f_2(\epsilon) = 1$$

$$\cos 2\phi_0 = \frac{1}{3}$$

$$\sin 2\phi_0 = 0.943$$

$$\sin^2 \phi_0 = 0.333$$

$$\cos 2\phi = \frac{3 - C_3}{\sqrt{\frac{2}{1 - \frac{1 - C_3}{2} \sin^2 2\phi}} + 3 + C_3}$$

and

$$\eta = \frac{E_s}{E} \frac{0.943}{\sin 2\phi} \frac{2 \sqrt{1 - \frac{1 - C_3}{2} \sin^2 2\phi} + 2 [1 + 2 \sin^2 \phi - (1 - C_3) \cos^2 \phi]}{5.33}$$

This value of  $\eta$  is plotted against stress in figure 1 for 24S-T aluminum alloy.

(b) For the case of clamped edges,

$$\epsilon = \infty$$

$$f_1(\epsilon) = 5.14$$

$$f_2(\epsilon) = 1.24$$

$$\cos 2\phi_0 = 0.26$$

$$\sin 2\phi_0 = 0.966$$

$$\sin^2 \phi_0 = 0.37$$

$$\cos 2\phi = \frac{1.24(3 - C_3)}{\sqrt{\frac{4.53}{1 - \frac{1 - C_3}{2} \sin^2 2\phi}} + 1.24(3 + C_3)}$$

and

$$\eta = \frac{E_S}{E} \frac{0.966}{\sin 2\phi} \frac{4.53 \sqrt{1 - \frac{1 - C_3}{2} \sin^2 2\phi} + 2.48 [1 + 2 \sin^2 \phi - (1 - C_3) \cos^2 \phi]}{8.84}$$

This value of  $\eta$  is nearly identical numerically with the value from case (a) and is represented by the same curve in figure 1.

Conditions under which Gerard's shear secant modulus applies.—  
Equation (1) gives the general formula for  $\eta$ , which involves, besides  $E_S/E$ , the following quantities:

$\left. \begin{array}{l} f_1(\epsilon) \\ f_2(\epsilon) \end{array} \right\}$	Functions only of restraint coefficient $\epsilon$
$\phi_0$	Angle of waves on assumption of elasticity (by equation (15)) depends only on $\epsilon$
$\phi$	Angle of waves in plastic range (by equation (13)) depends on $\epsilon$ and plasticity coefficient $C_3$
$C_3$	Plasticity coefficient

The magnitude of the restraint coefficient  $\epsilon$  is considered to be part of the data furnished with the problem. Thus,  $f_1(\epsilon)$  and  $f_2(\epsilon)$  are known constants; the angle  $\phi_0$  is therefore also a known constant. If, in addition to these quantities entering into equation (1), the plasticity coefficient  $C_3$  should also be a constant, equation (1) would reduce to the form

$$\eta = \text{Constant} \frac{E_S}{E}$$

Gerard's assumption is, from equation (2) of reference 3,

$$\eta = \frac{G_S}{G}$$

where the  $G's$  refer to the slope of a shear stress-strain curve derived from the axial stress-strain curve.

The plasticity coefficient  $C_3$  is defined as  $\frac{1}{2} + \frac{1}{2} \frac{E_t}{E_s}$  and therefore the condition for constancy of  $C_3$  is that

$$E_t = \chi E_s$$

or

$$\frac{d\sigma_1}{de_1} = \chi \frac{\sigma_1}{e_1}$$

where  $\chi$  is some constant. The relation  $\sigma_1 = Ke_1^\chi$ , where  $K$  is a constant, satisfies this requirement. For Gerard's curve for 24S-0 aluminum alloy,  $\chi$  is approximately 0.28 over the plastic range, and the requirement for a constant  $C_3$  is closely fulfilled. When the value of  $\eta$  is computed from equation (1) it is found that  $\eta = 0.89 \frac{E_s}{E}$ . This relation is plotted as the solid line in figures 2 and 3.

## REFERENCES

1. Stowell, Elbridge Z.: Critical Shear Stress for an Infinitely Long Flat Plate with Equal Elastic Restraints against Rotation along the Parallel Edges. NACA ARR No. 3K12, 1943.
2. Stowell, Elbridge Z.: A Unified Theory of Plastic Buckling of Columns and Plates. NACA TN No. 1556, 1948.
3. Gerard, George: Critical Shear Stress of Plates above the Proportional Limit. Jour. Appl. Mech., vol. 15, no. 1, March 1948, pp. 7-12.



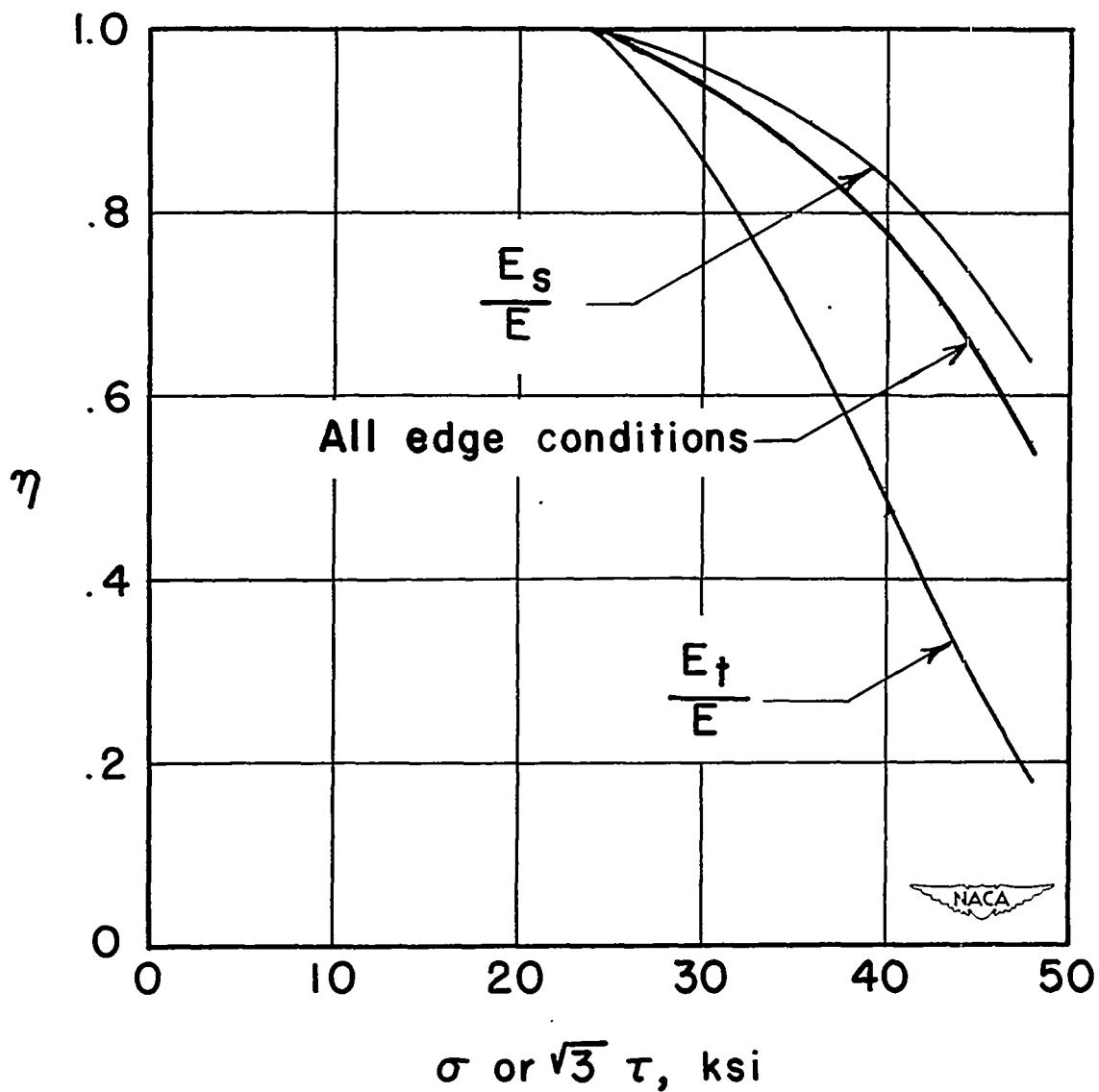


Figure 1.— Values of  $\eta$  for a long plate of 24S-T aluminum alloy under uniform shear stress. (The curves for  $E_s/E$  and  $E_t/E$  for compressive stress  $\sigma$  are included for comparison.)

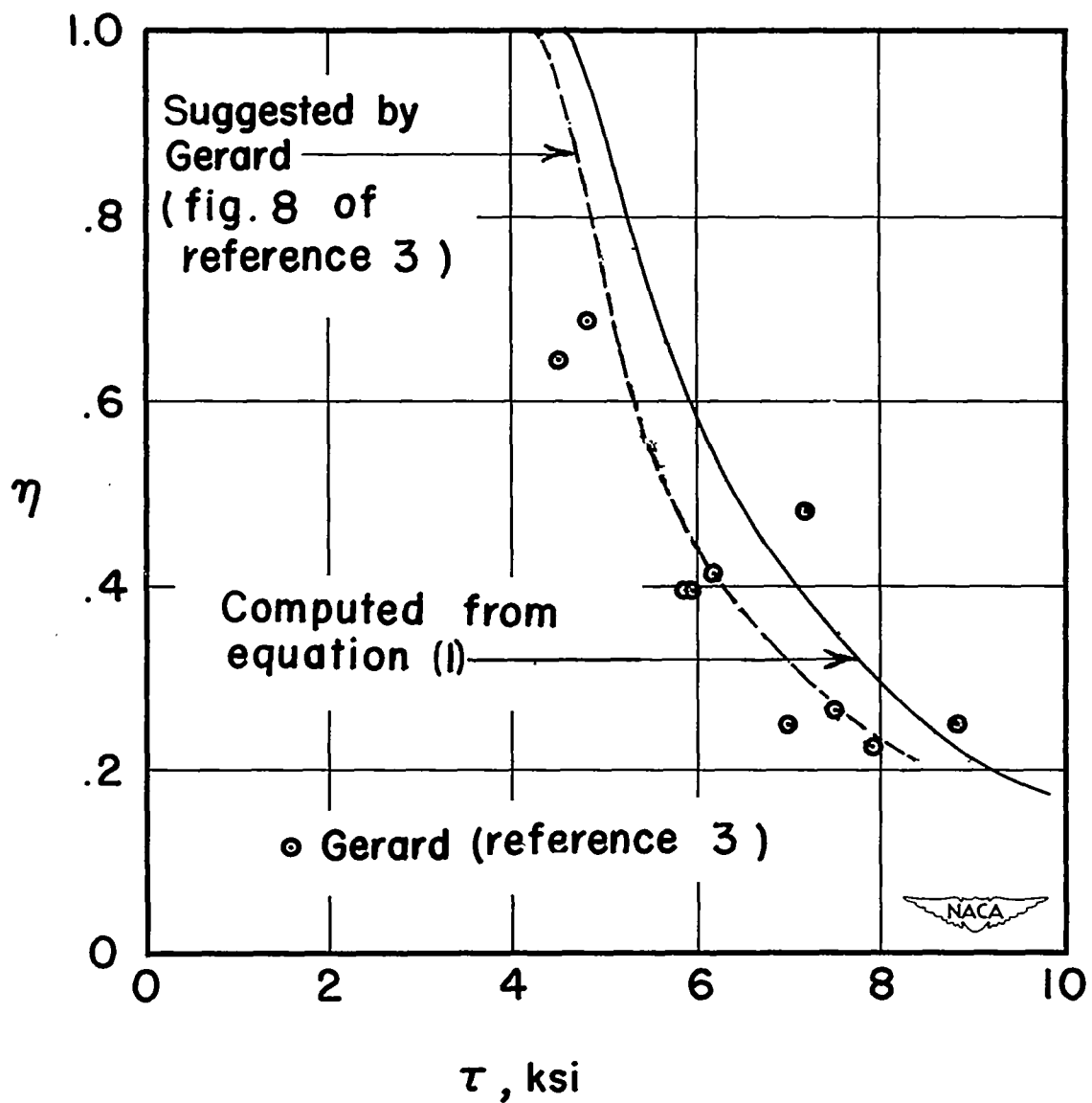


Figure 2.— Values of  $\eta$  for a long plate of 24S-O aluminum alloy under uniform shear stress.

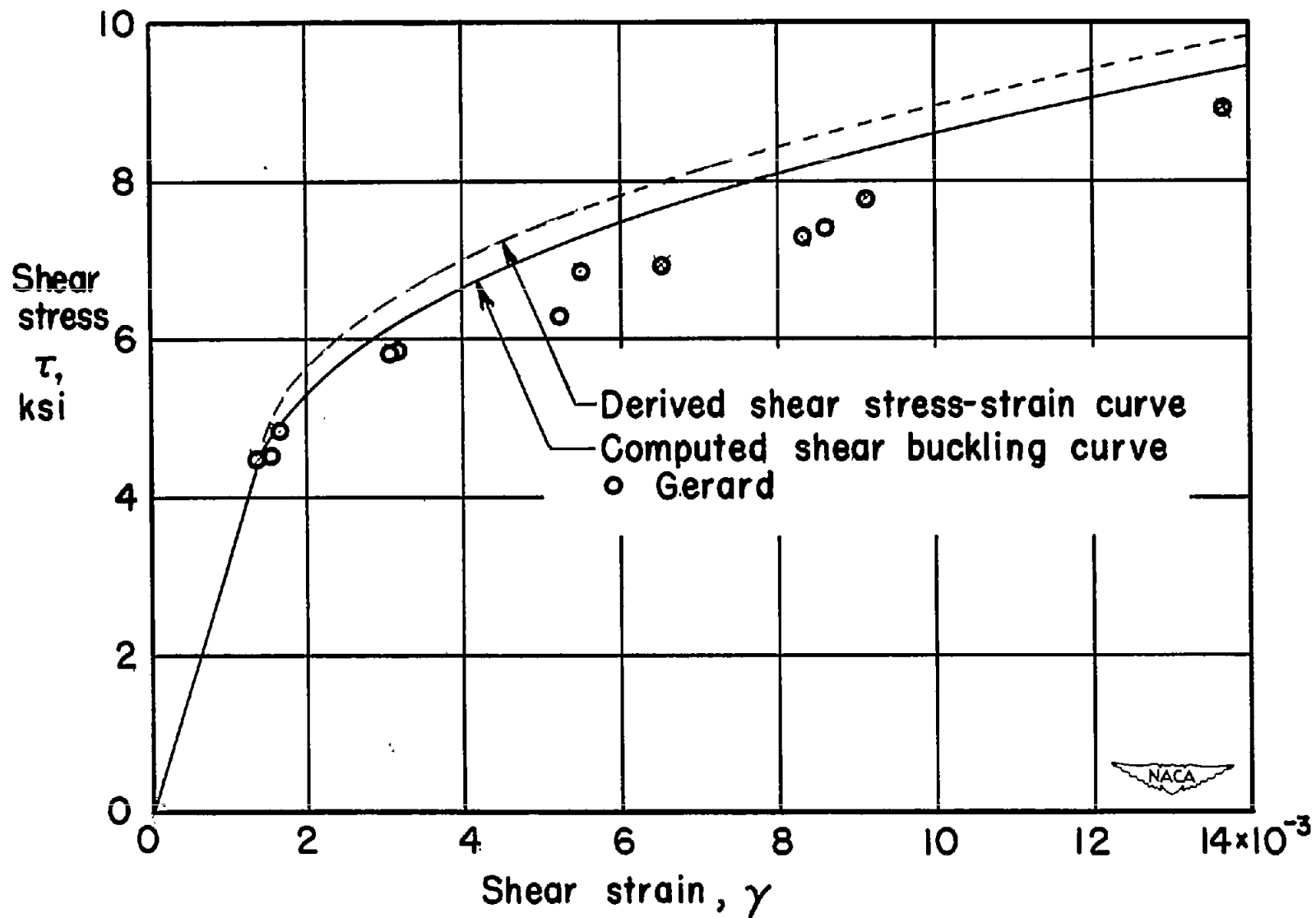


Figure 3.— Comparison of derived shear stress-strain curve and theoretical buckling curve with test data of Gerard.

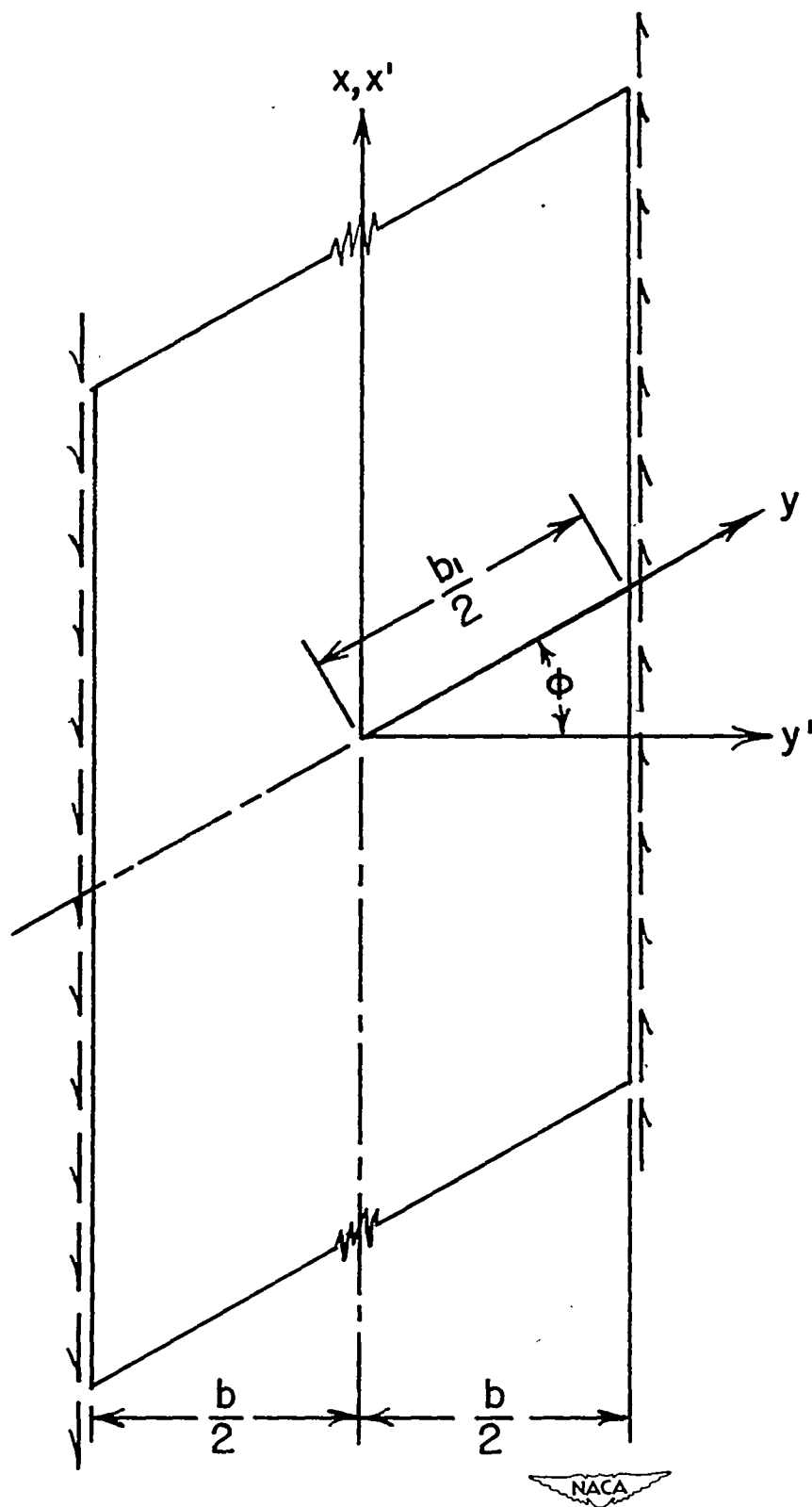


Figure 4.- Oblique coordinate system.